*J. Synchrotron Rad.* (1999). **6**, 918–927

# Membrane proteins: structure and function

**Tomitake Tsukihara* and Soo Jae Lee**

*Institute for Protein Research, Osaka University, 3-2 Yamadaoka, Suita, Osaka 565-0871, Japan. E-mail: tsuki@protein.osaka-u.ac.jp*

(*Received 29 March 1999; accepted 4 May 1999*)

Proteins residing in the lipid bilayer of a membrane surrounding a biological compartment make it possible for the compartment to engage in specialized functions. Since the determination of the X-ray structure of the bacterial photoreaction centre, high-resolution structures for more than 15 integral membrane proteins have been elucidated, mainly by X-ray and partly by electron diffraction methods. The energy-conversion systems, namely those involving photosynthesis and respiration, contain various kinds of integral membrane proteins. The transmembrane parts of these membrane proteins fold into $\alpha$-helices. Proton and electron transfer within the molecules have been inferred by inspecting the structures. Channels through which chemical substances are translocated selectively have important roles in various biological processes, such as mass transfer and signalling. Two structural architectures are known for the channels. One is an antiparallel $\beta$-barrel consisting of 14–22 strands and the other is $\alpha$-helical consisting of eight to ten $\alpha$-helices. Each channel has a structure suitable for selective transfer of a specific substance. Two types of anchoring architectures have been elucidated by the X-ray method. Prostaglandin H2 synthase-1 has helical anchors located with parallel orientation along and closely following the membrane surface. OmpA has an anchor domain arranged in the form of an antiparallel $\beta$-barrel consisting of eight strands.

**Keywords: membrane proteins; crystal structures; X-ray diffraction; electron diffraction; protein structures; protein functions.**

## 1. Introduction

Living things have various kinds of membranes surrounding the compartments. The compartments can enclose a cell, plasma, nucleus, endoplasmic reticulum, golgi apparatus, lysosome, peroxisome, endosome, mitochondrion, chloroplast, thylakoid *etc*. All biological membranes have a common structure, consisting of a thin film of about 50 Å in thickness and made up of lipid and protein molecules. Proteins attached to the membranes make it possible for the compartments to undertake specialized functions. The proteins are associated with membranes in different ways. Integral membrane proteins have a polypeptide segment which extends through, or is buried in, the lipid bilayer. They cannot be released from the membrane without detergents. Some membrane proteins that do not extend into the lipid bilayer are bound to the membrane by non-covalent interaction with the integral membrane proteins. These proteins are referred to as peripheral membrane proteins, which can be released from the membrane by more gentle procedures than integral membrane proteins. The other membrane proteins are bound to the lipid bilayer by covalent linkage, which anchors the protein to the membrane. These proteins are as hydrophilic as a water-soluble protein and can be released by cleaving a covalent bond between the protein and a fatty acid molecule.

We have previously reviewed the structural features of the integral membrane proteins determined at high resolution by X-ray and electron crystallographic methods (Sakai & Tsukihara, 1998). The membrane proteins play key roles in various biological processes. The integral membrane proteins are classified into three categories, namely monotopic, bitopic and polytopic, according to their membrane-spanning topology as shown in Fig. 1 (Blobel, 1980). Although the known structures of membrane proteins are few compared with those of water-

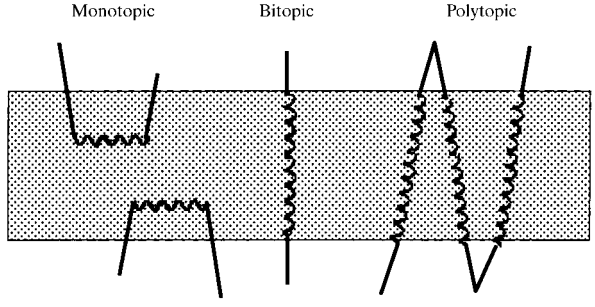


**Figure 1**
Classification of integral membrane proteins as monotopic, bitopic and polytopic (Blobel, 1980). The lipid bilayer of the biological membrane is indicated by the grey belt. The polypeptide segments in the membrane for the monotopic and the bitopic proteins are $\alpha$-helices as far as their structures are known. Those for the polytopic proteins are $\alpha$-helix or $\beta$-structure.

soluble proteins, a close analysis of each of the structures allows us to understand more deeply the molecular mechanism of how membrane proteins function. The structure–function relationships of the integral membrane proteins so far determined by X-ray and electron crystallographic methods are described in this paper.

## 2. Membrane proteins in solar energy conversion systems

Although chemical substances making up food are the immediate source of energy, the ultimate energy source for most living things is light. Plants and some bacteria fix light energy by employing several protein-pigment complexes arranged in membranes. Reaction centres (RCs) are the sites of energy conversion where light-induced charge separation takes place. Crystal structure determination of the RC of *Rhodopseudomonas viridis*, a photosynthetic bacterium, was a seminal event in stimulating X-ray crystallographic studies of membrane proteins (Deisenhofer *et al.*, 1984). Light-harvesting complexes, which collect solar energy and transfer it efficiently to the RCs, are the other protein-pigment complexes that make up photosynthetic membranes.

The three-dimensional structure of *R. viridis* RC has been refined at 2.3 Å resolution (Deisenhofer *et al.*, 1995). The RC consists of four protein subunits, L, M, H and cytochrome with four c-type heme groups. Other prosthetic groups are four bacteriochlorophyll (Bch) *b*, two bacteriopheophythin (Bph) *b*, two quinones, one non-heme ferrous iron and one carotenoid. The structures of the L, H and M subunits, as well as those of the prosthetic groups, are illustrated in Fig. 2. Electrons of Bch molecules excited by solar energy are transferred to an exchangeable quinone *via* Bch *b*, Bph *b* and tightly bound quinone to generate charge separation within the complex. The quinone, with high-energy electrons, reduces cytochrome *b6-f*, a photosynthetic complex, producing a proton gradient across the membrane. In addition to the RCs of *R. viridis* (Deisenhofer *et al.*, 1984, 1985, 1995) and *Rhodobactor sphaeroides* (Allen *et al.*, 1987; Ermler *et al.*, 1994), the X-ray structures of bacterial antenna complexes (LH2) from *Rhodopseudomonas acidophila* (McDermott *et al.*, 1995) and *Rhodospirillum molischianum* (Koepke *et al.*, 1996) have been determined at resolutions of 2.5 and 2.4 Å, respectively. The cylindrical structure of LH2 from *R. acidophila* is depicted in Fig. 3. The transmembrane helices of nine $\alpha$-proteins are packed side by side to form a cylinder with a radius of 18 Å. The nine helical $\beta$-apoproteins are arranged radially with the $\alpha$-apoproteins to form an outer cylinder with a radius of 34 Å. Both subunits are small proteins comprising of about 50 amino acid residues. The light-absorbing pigments, Bch *a* and carotenoids, are non-covalently bound to the $\alpha$- and $\beta$-apoproteins. The structure of

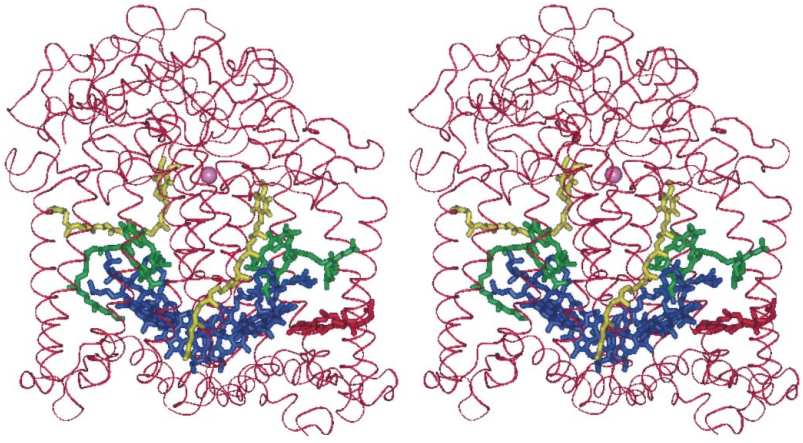

**Figure 2**
A stereoview of the *R. sphaeroides* RC (PDB code 1PCR; Ermler *et al.*, 1994). Subunits L, M and H are drawn as ribbons. Prosthetic groups for Bch *b* (blue), two Bph *b* (green), two quinones (yellow), one non-haem iron (pink) and one carotenoid (red) are drawn as ball-and-sticks. The prosthetic groups are well arranged for energy transfer among these groups.

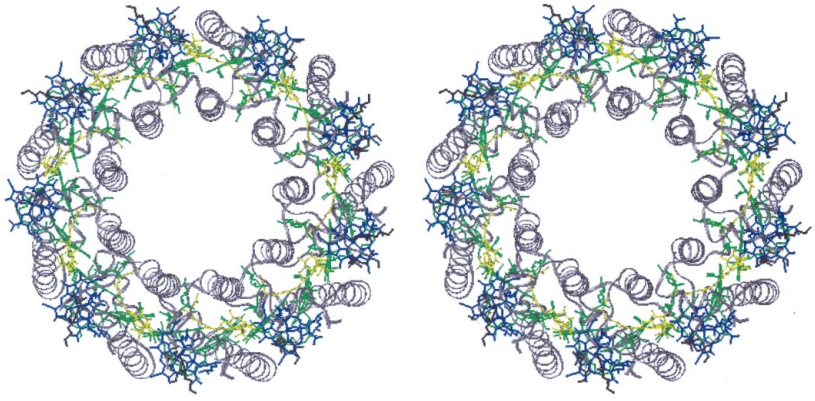

**Figure 3**
A stereoview of *R. acidophila* LH2 is shown as ribbons for protein subunits and as ball-and-sticks for prosthetic groups (PDB code 1KZU; McDermott *et al.*, 1995). LH2 is a nonameric complex, each monomer consisting of two protein subunits of $\alpha$ and $\beta$, and two vertically oriented Bch *a* (green), a horizontally oriented Bch *a* (blue) and carotenoid (yellow). The solar energy is absorbed efficiently by these prosthetic groups.

*R. molischianum* LH2 exhibits cylindrical architecture similar to that of *R. acidophila* LH2. The *R. molischianum* LH2 is an $\alpha\beta$-octamer in contrast to a nonamer for the *R. acidophila* LH2.

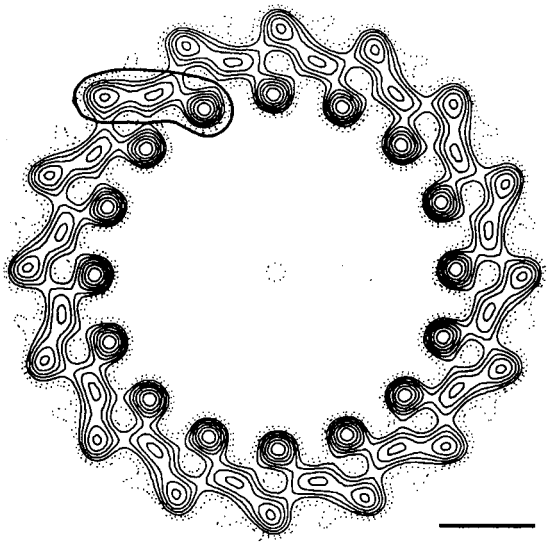

**Figure 4**
8.5 Å projection map of LH1 by the electron-diffraction method. The complex consists of 16 monomers, each with $\alpha$ and $\beta$ proteins and prosthetic groups. 16 pairs of the inner and outer peaks correspond to $\alpha$ and $\beta$ proteins, respectively. The ring with a 68 Å inner radius can accommodate the RC. The scale bar represents 20 Å. The figure is reproduced from Karrasch *et al.* (1995) with permission.

The 8.5 Å projection map of the light-harvesting complex I (LH1) of *Rhodospirillum rubrum* obtained by electron crystallographic methods shows 16 $\alpha\beta$-subunits in a 116 Å outer-diameter ring with a 68 Å hole in the centre, as shown in Fig. 4 (Karrasch *et al.*, 1995). LH1 can accommodate an RC molecule in the hole. Fig. 5 is a schematic diagram showing the arrangement of the antenna complexes, LH1 and LH2, and RC, and the flow of excitation energy in the photosynthetic membrane (Kuhlbrandt, 1995). The well organized arrangement allows the cell to achieve high efficiency in solar energy conversion.

Plants as well as cyanobacteria have another solar energy conversion system in the photosynthetic membrane. The light-harvesting chlorophyll a/b-protein complex (LHC-II) associated with photosystem II is involved in plant-type photosynthesis. The structure of LHC-II was determined at 3.4 Å resolution by electron crystallography of a two-dimensional crystal (Kuhlbrandt *et al.*, 1994) prior to crystal structure analyses of the bacterial light-harvesting antenna complexes, LH1 and LH2. Each apoprotein of 232 amino acids has three transmembrane $\alpha$-helices binding 12 chlorophylls and two carotenoids. The X-ray structure of photosystem I (PSI) of *Synechococcus elongatus* was determined at 4 Å resolution (Krauss *et al.*, 1996). The PSI with a trimeric structure has 31 transmembrane $\alpha$-helices and light-harvesting pigments in the monomer. The structural model reveals a joint photosynthetic RC and light-harvesting antenna system. Higher-resolution analysis of the PSI as well as that of PSII are awaited with great interest.

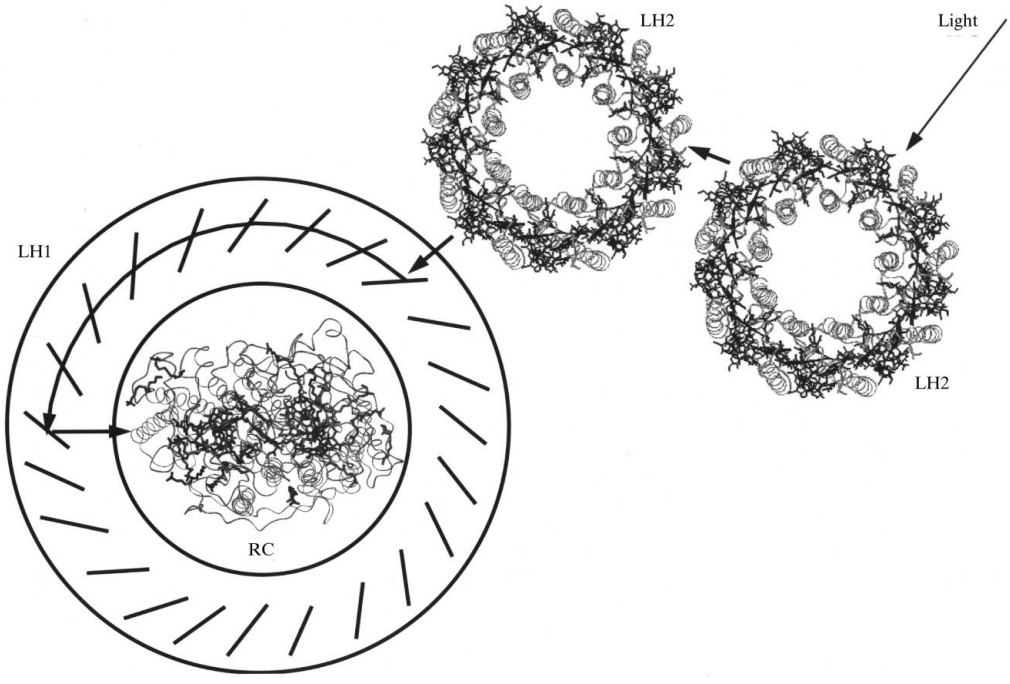


**Figure 5**
Schematic drawing showing the flow of energy excited by light in a bacterial photosynthetic system. The energy absorbed by LH2 spreads through the ring arrangement of Bch pigments. The energy is transmitted sequentially to adjacent LH2, LH1 and finally to RC. The picture is reproduced by modifying Fig. 4 of Kuhlbrandt (1995) with permission.

Halobacteria utilize solar energy by a different process from photosynthesis. Bacteriorhodopsin, a protein residing in the cell membrane, pumps protons from the cytoplasm to the extra cellular space to generate a proton gradient which is used for ATP synthesis. Several atomic coordinates of the membrane protein, determined by X-ray and electron crystallographic methods, have been deposited in the Protein Data Bank (PDB) (Bernstein *et al.*, 1977; Abola *et*

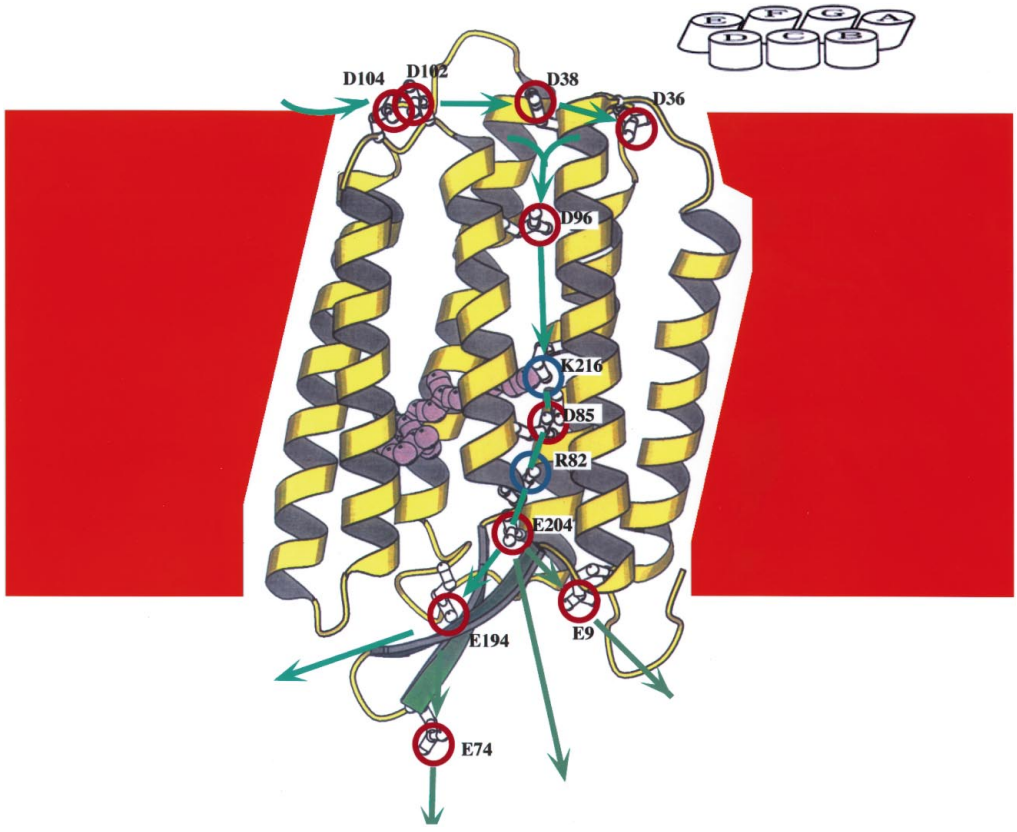


**Figure 6**
Possible proton pathway in bacteriorhodopsin. Polypeptide folding is drawn as ribbons. The space-filling model coloured purple is a retinal. Aspartic acids, lysine, arginine and glutamic acids which are included in proton translocation are shown by ball-and-sticks and single letter notation with a residue number. The arrays represent proton flows in the molecule. The red belt indicates the membrane region. The seven cylinders at the top right represent the arrangement of the helices. The figure is reproduced from Kimura (1999) with permission.

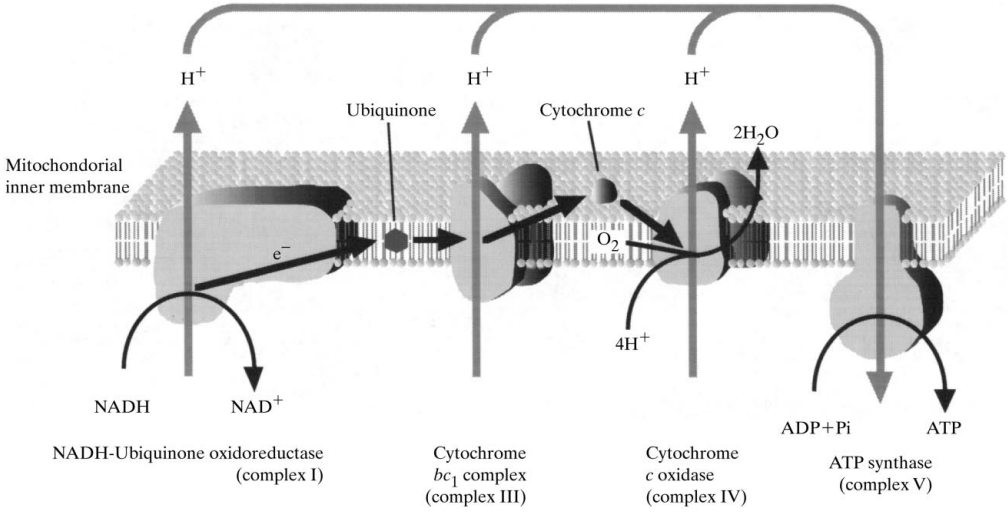


**Figure 7**
Schematic drawing of respiratory complexes in the mitochondrial inner membrane. The upper and lower sides are intermembrane and matrix spaces, respectively. Electrons and protons originating from food are used by the complexes to accumulate protons in the intermembrane space. The ATP synthase is driven by the proton chemical potential to synthesize ATP from ADP in the matrix space.

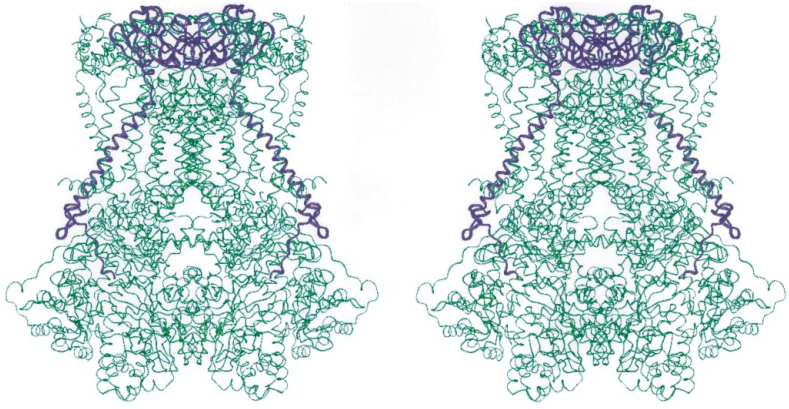

**Figure 8**
Stereoview of a dimeric structure of cytochrome *bc* complex (PDB code 1BCC; Zhang *et al.*, 1998). Rieske proteins are depicted by heavy purple ribbons and the other subunits by thin green ribbons. A transmembrane $\alpha$-helix of the Rieske protein interacts tightly with transmembrane helices belonging to one monomer, while the Fe–S domain of the Rieske protein is in close contact with the other monomer.

*al.*, 1987). Three structural models of the transmembrane region consisting of seven $\alpha$-helices coincide well with one another, despite some conformational differences on both sides of the membrane among these models (Grigorieff *et al.*, 1996; Pebay-Peyroula *et al.*, 1997; Kimura *et al.*, 1997). A possible pathway of the proton in bacteriorhodopsin of *Halobacterium salinarium* is shown in Fig. 6 (Kimura *et al.*, 1997). A chromophore, retinal in an all-*trans* conformation, is attached to protonated Lys216 by a Schiff base. Once light is absorbed, the retinal is isomerized from all-*trans* to the 13-*cis* conformation. This isomerization facilitates proton translocation from Lys216 to Asp 85, followed by the release of a proton to the extra cellular space *via* Glu204. Then, Lys216 accepts a proton from Asp96, and 13-*cis* retinal is converted to an all-*trans* conformation to form the Schiff base with Lys216. The proton pumping cycle is concluded by proton transfer from the cytoplasmic space to Asp96 (Henderson *et al.*, 1990; Kimura *et al.*, 1997).

## 3. Membrane proteins of the respiratory chain

Mitochondria, which are present in all eucaryotic cells and some bacteria, convert energy from chemical fuels into the useful form of ATP. Respiratory enzyme complexes residing in the mitochondrial inner membrane are shown in Fig. 7. The X-ray structures of complexes III, cytochrome bc1, have been determined independently by three groups (Xia *et al.*, 1997; Zhang *et al.*, 1998; Iwata *et al.*, 1998). The cytochrome bc1 transfers electrons from an ubiquinol to a soluble cytochrome *c* in the intermembrane space and pumps protons from the matrix space to the intermembrane space to create a proton chemical potential. Bovine heart cytochrome bc1 complex is a dimer, with each monomer made up of 11 different subunits. Each monomer contains four redox centres, consisting of two heme groups, $b_H$ and $b_L$ of cytochrome *b*, one heme group in cytochrome $c_1$ and one Fe–S cluster of Rieske protein, as shown in Fig. 8.

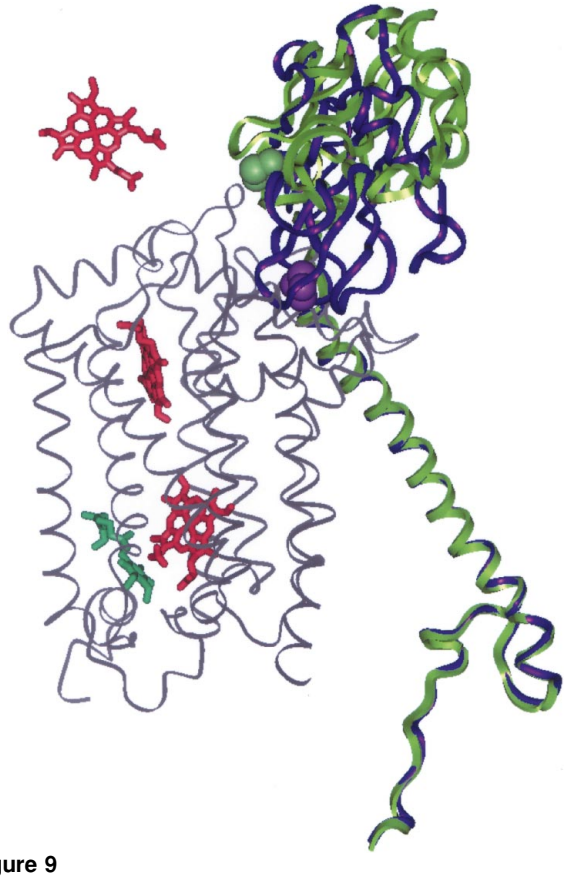

**Figure 9**
Isolated close-up view of the two conformational states of the Rieske protein (PDB codes 1BCC and 3BCC; Zhang *et al.*, 1998). The iron–sulfur cluster in one conformation (purple) is in contact with the cytochrome *b* (black) with two heme group (red) and stigmatellin (green at the bottom), while the Fe–S cluster in the other conformational state (green) is located closely to the heme group (red at the top) of cytochrome $c_1$.

X-ray structures of the complex III in both the presence and absence of inhibitors of quinone oxidation reveal two different locations for the Fe–S domain of the Rieske

protein (Fig. 9). One location of the Fe–S cluster is close enough to the supposed quinol oxidation site to allow reduction of the Fe–S cluster by the ubiquinol. The other site of the Fe–S cluster is close enough to the heme group of cytochrome $c_1$ to allow oxidation of the Fe–S cluster by the cytochrome $c_1$. Novel mechanisms for internal electron transfer, whereby large displacement of the Fe–S domain of Rieske protein shuttles electrons from ubiquinol to cytochrome $c_1$, have been proposed (Zhang *et al.*, 1998; Iwata *et al.*, 1998).

Cytochrome *c* oxidase is a key enzyme in the respiratory chain. The enzyme catalyzes a reaction in which dioxygen reduction by protons and electrons from cytochrome is coupled to proton pumping across the mitochondrial or bacterial membrane. The enzyme drives protons about 50 Å across the membrane against an electrochemical gradient to accumulate protons on one side of the membrane. The X-ray structures of cytochrome *c* oxidase have been determined for the 13-subunit bovine heart oxidase (Tsukihara *et al.*, 1995, 1996: Yoshikawa *et al.*, 1998; Tomizaki *et al.*, 1999) as well as for the four-subunit oxidase from the bacterium *Paracoccus denitrificans* (Iwata *et al.*, 1995; Ostermeier *et al.*, 1997). The structures of subunits I, II and III are very similar in both molecules. Locations of metal centres and a close-up structure of the dioxygen reduction site is presented in Fig. 10. An electron accepted at CuA is transferred to heme *a* through the hydrogen-bond network between propionic groups of heme *a* and CuA centre, and to heme $a_3$ through a bridging peptide of His–Phe–His between hemes *a* and $a_3$. Dioxygen is held between $Fe_{a3}$ and CuB, coordinated by three histidine residues. The 2.3 Å X-ray structures have revealed that His240 ligating to CuB is covalently bound to a Tyr244 (Yoshikawa *et al.*, 1998). The covalent linkage presumably allows electron transfer from the CuB to a dioxygen molecule in conjunction with protonation of the dioxygen molecule by a hydroxyl group of Tyr244 pointing to the dioxygen reduction site. A proton pumping mechanism, shown in Fig. 11, has been proposed by structural comparison between the oxidized and the reduced states of bovine enzyme (Yoshikawa *et al.*, 1998). Before the X-ray structures appeared, another proton pumping mechanism was proposed involving a histidine cycle in which one of the imidazole ligands to CuB changes its conformation and protonation state, depending on the oxidation state of the dioxygen reduction site (Wikstrom *et al.*, 1994). The X-ray

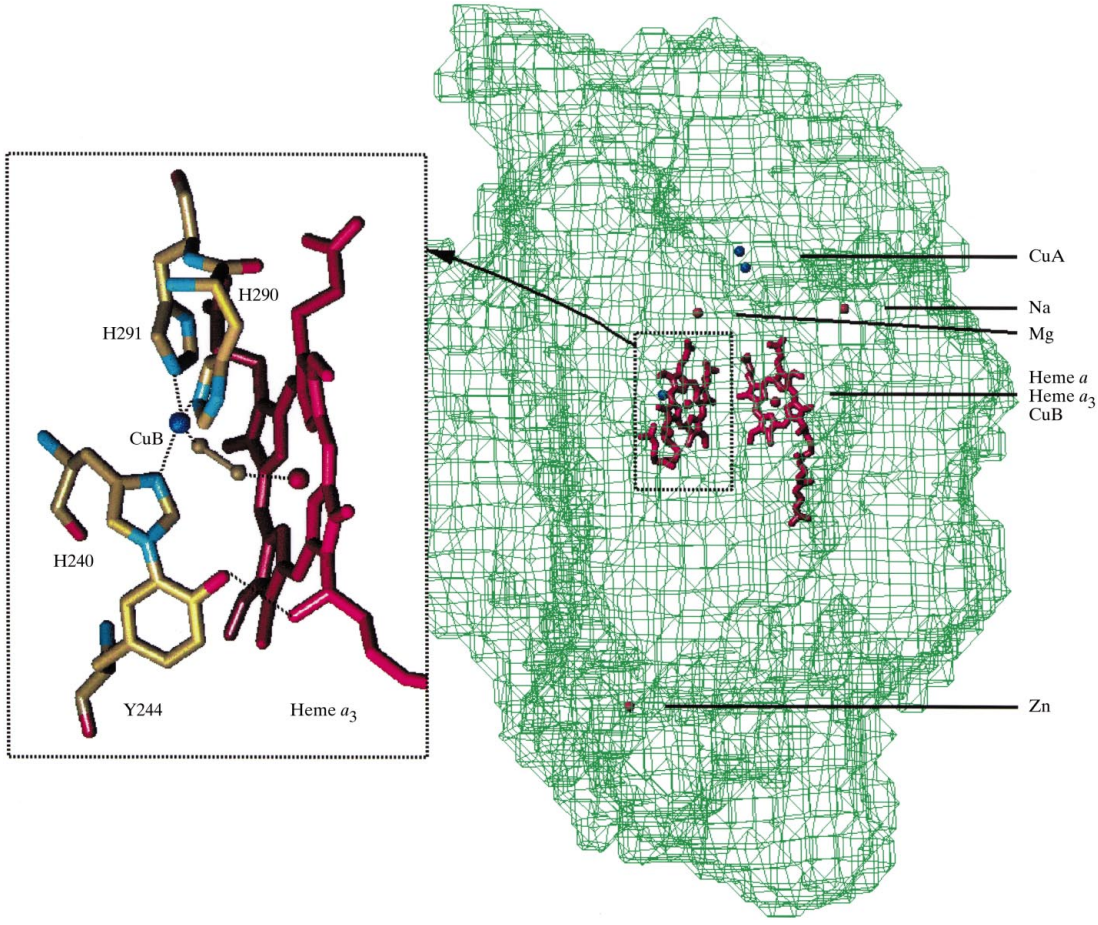


**Figure 10**
Location of the metal centres and molecular surface of bovine cytochrome *c* oxidase, and close-up structure of the dioxygen reduction site (PDB code 2OCC; Yoshikawa *et al.*, 1998). Dioxygen is held between $Fe_{a3}$ and CuB. A covalent bond between His240 and Tyr244 is formed by post-translational modification.

structure of the bacterial enzyme showed that one of the imidazole ligands lost electron density in the Fourier map at 2.8 Å resolution (Iwata *et al.*, 1995). The histidine residue was assigned as the site of proton pumping (Iwata *et al.*, 1995). Several pathways have been suggested as candidates for proton translocations (Iwata *et al.*, 1995; Tsukihara *et al.*, 1996). These structural studies should enable us to plan further spectroscopic and site-directed mutagenesis experiments.

## 4. Membrane proteins forming channels

Each biological membrane is equipped with various channels that aid in the selective transport of molecules or ions across the membrane. Porins in the outer membranes of gram-negative bacteria, mitochondria and chloroplast act as molecular sieves for hydrophilic molecules smaller than ~600 Da. The X-ray structures of porin from *Rhodobacter capsulatus* (Weiss, Abele *et al.*, 1991; Weiss, Kreusch *et al.*, 1991; Weiss & Schulz, 1992), matrix porin (OmpF) from *Escherichia coli* (Cowan *et al.*, 1992) and phosphoporin (PhoE) from *E. coli* (Cowan *et al.*, 1992) have revealed 16- to 18-stranded antiparallel $\beta$-barrels, each forming a pore that facilitates the diffusion of small hydrophilic molecules. Fig. 12 is a ribbon drawing of *R. capsulatus* porin. The pore is constricted by an internal loop structure to prevent molecules larger than 600 Da from passing through the pore. Similar antiparallel $\beta$-barrels have been shown by X-ray analyses of maltoporin (LamB), a protein that facilitates the diffusion of maltodextrins across the outer membrane of the gram-negative bacterium *Staphylococcus aureus* (Schirmer *et al.*, 1995), and a sucrose-specific porin (ScrY) from *Salmonella typhimurium* (Forst *et al.*, 1998). Microbial toxins such as $\alpha$-hemolysin ($\alpha$HL) and aerolysin can form transmembrane channels that destroy cells by breaking their permeability barriers against ions, water and small molecules. Figs. 13(*a*) and 13(*b*) are the monomeric and heptameric structures of $\alpha$HL, respectively (Song *et al.*, 1996). A stem consisting of a 14-stranded antiparallel $\beta$-barrel forms a transmembrane channel. $\alpha$HL and *Aeromonas hydrophila* aerolysin (Parker *et al.*, 1994) are transmembrane pores with antiparallel $\beta$-barrels in an oligomeric state. The proteins are water-soluble in the monomeric form.

The structure of FhuA, the receptor for ferrichrome-iron in *Escherichia coli* outer membrane which mediates the active transport of ferric siderophores across the outer membrane, was determined by the X-ray method (Ferguson *et al.*, 1998). It is an antiparallel $\beta$-barrel channel consisting of 22 antiparallel $\beta$-strands, as shown in Fig. 14. A structurally distinct domain located in the barrel constricts to regulate a selective iron transport across the outer membrane.

Potassium ions diffuse rapidly across cell membranes through potassium channels. All of the potassium channels show a high selectivity toward $K^+ \approx Rb^+ > Cs^+$, while permeabilities for the smaller alkaline ions $Na^+$ and $Li^+$ are very low at around 0.01 to 0.02 of that of $K^+$ (Hille, 1973). The potassium channel from *Streptomyces lividans*, an integral membrane protein, is a tetramer with a fourfold symmetry about a central pore, as shown in Fig. 15. Each

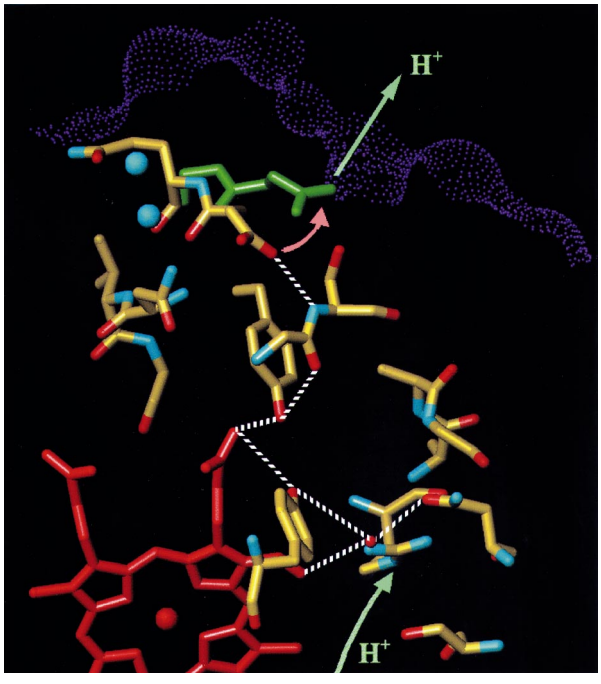


**Figure 11**
Proton pumping mechanism of the bovine cytochrome *c* oxidase inferred by conformational change upon reduction of the enzyme. The surface of the molecule is represented by blue dots. The carboxyl group of Asp51 must be protonated inside the molecule in the oxidized state. The structure in the reduced state is coloured in green. The side chain is exposed to the molecular surface to release a proton upon reduction. Protons are supplied from the matrix space along hydrogen-bond networks shown by white broken lines (Yoshikawa *et al.*, 1998).

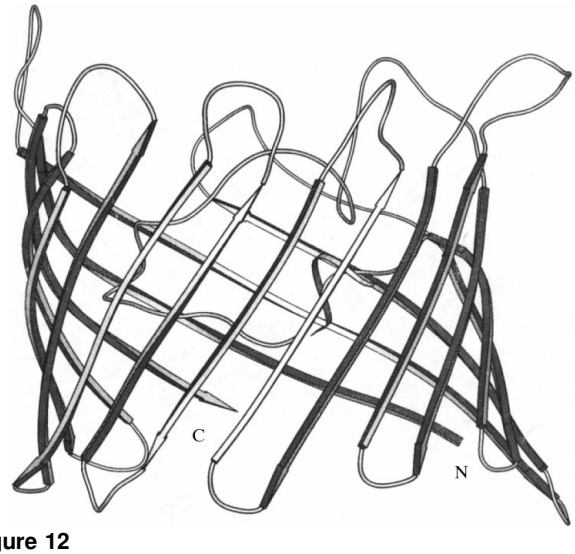


**Figure 12**
A ribbon drawing of *R. capsulatus* porin (PDB code 1PRN; Weiss & Schulz, 1992).

subunit consists of a six-turn outer helix, a three-turn pore helix and an eight-turn inner helix (Doyle *et al.*, 1998). A potassium ion which is identified in the pore is coordinated by eight carbonyl groups with rigid conformation. The ion is dehydrated when it enters the pore. The coordination geometry around the potassium ion of ionic radius 1.33 Å is designed so that dehydration energy is compensated by the interaction between the potassium ion and carbonyl groups, whereas the structure of the carbonyl groups cannot compensate for the dehydration energy for highly hydrated sodium ions with an ionic radius of 0.98 Å. Thus, the channel transfers potassium ions selectively. The X-ray structure determination of a gated mechanosensitive ions channel from *Mycobacterium tuberculosis* was reported following publication of the potassium channel (Chang *et al.*, 1998). This channel is a homopentamer, with each subunit containing two transmembrane $\alpha$-helices and a third cytoplasmic $\alpha$-helix. A channel gate was identified at the cytoplasmic side of the pore.

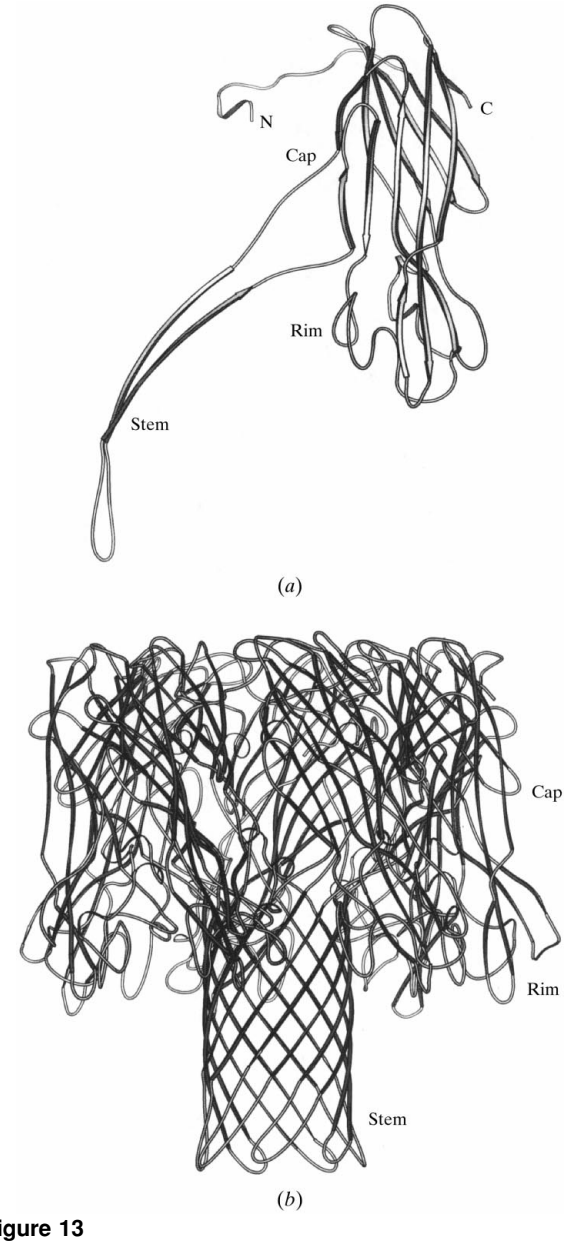


**Figure 13**
Ribbon drawings of (*a*) the $\alpha$HL monomer and (*b*) the $\alpha$HL heptamer (PDB code 7AHC; Song *et al.*, 1996).

## 5. Other integral membrane proteins

Prostaglandin H2 synthase-1 is the only integral monotopic membrane protein whose crystal structure has been determined thus far (Picot *et al.*, 1994). Anchor helices are embedded in a shallow membrane. The helices are roughly parallel to the membrane surface with the hydrophobic residues facing the inside of the membrane and the rather hydrophilic residues situated at the surface region. Since the amphipathic helices are not the most hydrophobic segments along the polypeptide chain, membrane segments expected from the amino acid sequence are incompatible with the crystal structure.

The X-ray structure of the N-terminal domain of the outer membrane protein A (OmpA) of *E. coli* showed that the domain forms an antiparallel $\beta$-barrel as in the case of the other outer membrane proteins (Pautsch & Schulz, 1998). The barrel consists of eight strands that appear to be constructed in the form of an inverse micelle with a hydrophilic cavity without forming a pore. The $\beta$-barrel anchors the C-terminal domain, consisting of residues 172 to 325, to the outer membrane. If a $\beta$-structure has to be

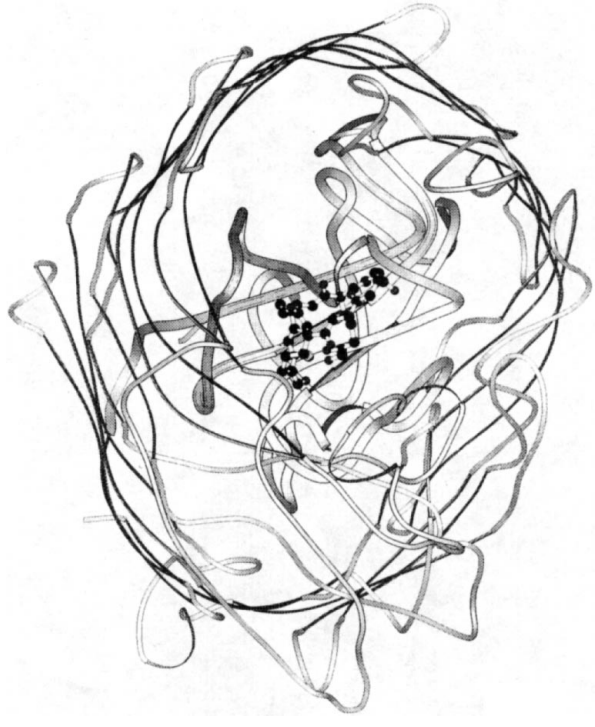

**Figure 14**
FhuA-ferrichrome-iron complex (PDB code 1FCP; Ferguson *et al.*, 1998). The protein structure is drawn as ribbons and the ferrichrome is represented by ball-and-sticks. FhuA is composed of a $\beta$-barrel domain formed by 22 antiparallel $\beta$-strands and a cork domain, which fills the barrel interior.

used, as is probably the case with the outer membrane proteins, the slim eight-stranded $\beta$-barrel seems to be an efficient construction for an anchor (Pautsch & Schulz, 1998).

## 6. Concluding remarks

The membrane proteins of bioenergetic systems, including bacterial RCs, bacterial LH2, plant LHCII, bacteriorhodopsin, cytochrome $bc_1$ and cytochrome $c$ oxidase, fold in the form of $\alpha$-helices in the transmembrane region. High-resolution structures of these membrane proteins have opened up a new era in molecular bioenergetics.

Each biological membrane has various kinds of membrane proteins functioning as channels. X-ray crystallography has elucidated two structural types of channels. One of them is the $\beta$-barrel channel, consisting of 14 to 22 antiparallel $\beta$-strands, exemplified by porin, OmpF, PhoE, LamB, ScrY and FhuA, while the other has a helical architecture, consisting of eight to ten transmembrane $\alpha$-helices, represented by the potassium channel and the large-conductance mechanosensitive channel. The structures of the channels determined by the X-ray crystallographic method have given us invaluable insight into the mechanism of molecular transport through membranes.

There are many unknown structures that still remain to be determined, particularly membrane proteins that play key roles in important biological processes, such as energy conversion, molecular transport, signalling and so on. Despite the many difficulties that one still encounters in the production, purification and crystallization of proteins, the number of crystal structures of membrane proteins determined each year is gradually increasing. Development of synchrotron radiation techniques should enable X-ray analysis of poor crystals that diffract weakly or a small crystal with dimensions of 20–40 μm by 20–40 μm by 5 μm (Pebay-Peyroula *et al.*, 1997). Synchrotron X-ray crystallography, coupled with developments in biochemical techniques, should facilitate structural studies of membrane proteins, leading to further progress in the understanding of biological processes.

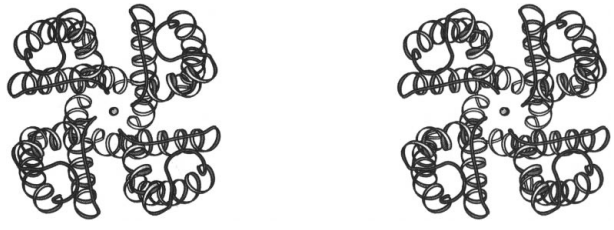

**Figure 15**
Stereoscopic drawing of the potassium channel of *S. lividans* looking along a fourfold symmetry axis (PDB code 1MSL; Chang *et al.*, 1998). A potassium iron on the fourfold axis is surrounded by eight carbonyl groups of the main chain segments, each next to the pore helix.

This research was supported in part by a Grant-in-Aid for the 'Research for the Future' program from the Japan Society for Promotion of Science (JSPS-RFTF96L00503 to TT). TT is a senior visiting scientist of RIKEN.

## References

Abola, F. C., Bernstein, F. C., Bryant, S. H., Koetzle, T. F. & Weng, J. (1987). Crystallographic Databases-Information Content, Software Systems, Scientific Applications, Data Commission of the International Union of Crystallography, Bonn, Cambridge, Chester, pp. 107–132.
Allen, J. P., Feher, G., Yeates, T. O., Komiya, H. & Rees, D. C. (1987). *Proc. Natl Acad. Sci. USA*, **84**, 6162–6166.
Bernstein, F. C., Koetzle, T. F., Williams, G. J., Meyer, E. E. Jr, Brice, M. D., Rodgers, J. R., Kennard, O., Shimanouchi, T. & Tasumi, M. (1977). *J. Mol. Biol.* **112**, 535–542.
Blobel, G. (1980). *Proc. Natl Acad. Sci. USA*, **77**, 1496–1500.
Chang, G., Spencer, R. H., Lee, A. T., Barclay, M. T. & Rees, D. C. (1998). *Science*, **282**, 2220–2226.
Cowan, S. W., Schirmer, T., Rummel, G., Steiert, M., Ghosh, R., Pauptit, R. A., Jansonius, J. N. & Rosenbusch, J. P. (1992). *Nature (London)*, **358**, 727–733.
Deisenhofer, J., Epp, O., Miki, K., Huber, R. & Michel, H. (1984). *J. Mol. Biol.* **180**, 385–398.
Deisenhofer, J., Epp, O., Miki, K., Huber, R. & Michel, H. (1985). *Nature (London)*, **318**, 618–624.
Deisenhofer, J., Epp, O., Sinning, I. & Michel, H. (1995). *J. Mol. Biol.* **246**, 429–457.
Doyle, D. A., Cabral, J. M., Pfuetzner, R. A., Kuo, A., Gulbis, J. M., Cohen, S. L., Chait, B. T. & MacKinnon, R. (1998). *Science*, **280**, 69–77.
Ermler, U., Fritzsch, G., Buchanan, S. K. & Michel, H. (1994). *Structure*, **2**, 925–936.
Ferguson, A. D., Hofmann, E., Coulton, J. W., Diederichs, K. & Welte, W. (1998). *Science*, **282**, 2215–2220.
Forst, D., Welte, W., Wacker, T. & Diederichs, K. (1998). *Nat. Struct. Biol.* **5**, 37–46.
Grigorieff, N., Ceska, T. A., Downing, K. H., Baldwin, J. M. & Henderson, R. (1996). *J. Mol. Biol.* **259**, 393–421.
Henderson, R., Baldwin, J. M., Ceska, T. A., Zemlin, F., Beckmann, E. & Downing, K. H. (1990). *J. Mol. Biol.* **213**, 899–929.
Hille, B. (1973). *J. Gen. Physiol.* **61**, 669–686.
Iwata, S., Lee, J. W., Okada, K., Lee, J. K., Iwata, M., Rasmussen, B., Link, T. A., Ramaswamy, S. & Jap, B. K. (1998). *Science*, **281**, 64–71.
Iwata, S., Ostermeier, C., Ludwig, B. & Michel, H. (1995). *Nature (London)*, **376**, 660–669.
Karrasch, S., Bullough, P. A. & Ghosh, R. (1995). *EMBO J.* **14**, 631–638.
Kimura, Y. (1999). *Proteins, Nucleic Acids, Enzymes*, **44**, 546–556. (In Japanese.)
Kimura, Y., Vassylyev, D. G., Miyazawa, A., Kidera, A., Matsushima, M., Mitsuoka, K., Murata, K., Hirai, T. & Fujiyoshi, Y. (1997). *Nature (London)*, **389**, 206–211.
Koepke, J., Hu, X., Muenke, C., Schulten, K. & Michel, H. (1996). *Structure*, **4**, 581–597.
Krauss, N., Schubert, W. D., Klukas, O., Fromme, P., Witt, H. T. & Saenger, W. (1996). *Nat. Struct. Biol.* **3**, 965–973.
Kuhlbrandt, W. (1995). *Structure*, **3**, 521–525.
Kuhlbrandt, W., Wang, D. N. & Fujiyoshi, Y. (1994). *Nature (London)*, **367**, 614–621.
McDermott, G., Prince, S. M., Freer, A. A., Hawthornthwaite-Lawless, A. M., Papiz, M. Z., Cogdell, R. J. & Isaacs, N. W. (1995). *Nature (London)*, **374**, 517–521.

Ostermeier, C., Harrenga, A., Ermler, U. & Michel, H. (1997). *Proc. Natl Acad. Sci. USA*, **94**, 10547–10553.
Parker, M. W., Buckley, J. T., Postma, J. P. M., Tucker, A. D., Leonard, K., Pattus, F. & Tsernoglou, D. (1994). *Nature (London)*, **367**, 292–295.
Pautsch, A. & Schulz, G. E. (1998). *Nat. Struct. Biol.* **5**, 1013–1017.
Pebay-Peyroula, E., Rummel, G., Rosenbusch, J. P. & Landau, E. M. (1997). *Science*, **277**, 1676–1681.
Picot, D., Loll, P. J. & Garavito, R. M. (1994). *Nature (London)*, **367**, 243–249.
Sakai, H. & Tsukihara, T. (1998) *J. Biochem. (Tokyo)*, **124**, 1051–1059.
Schirmer, T., Keller, T. A., Wang, Y. F. & Rosenbusch, J. P. (1995). *Science*, **267**, 512–514.
Song, L., Hobaugh, M. R., Shustak, C., Cheley, S., Bayley, H. & Gouaux, J. E. (1996). *Science*, **274**, 1859–1866.
Tomizaki, T., Yamashita, E., Yamaguchi, H., Aoyama, H., Tsukihara, T., Shinzawa-Itoh, K., Nakashima, R., Yaono, R. & Yoshikawa, S. (1999). *Acta Cryst.* D**55**, 31–45.
Tsukihara, T., Aoyama, H., Yamashita, E., Tomizaki, T., Yamaguchi, H., Shinzawa-Itoh, K., Nakashima, R., Yaono, R. & Yoshikawa, S. (1995). *Science*, **269**, 1069–1074.
Tsukihara, T., Aoyama, H., Yamashita, E., Tomizaki, T., Yamaguchi, H., Shinzawa-Itoh, K., Nakashima, R., Yaono, R. & Yoshikawa, S. (1996). *Science*, **272**, 1136–1144.
Weiss, M. S., Abele, U., Weckesser, J., Welte, W., Schiltz, E. & Schulz, G. E. (1991). *Science*, **254**, 1627–1630.
Weiss, M. S., Kreusch, A., Schiltz, E., Nestel, U., Welte, W., Weckesser, J. & Schulz, G. E. (1991). *FEBS Lett.* **280**, 379–382.
Weiss, M. S. & Schulz, G. E. (1992). *J. Mol. Biol.* **227**, 493–509.
Wikstrom, M., Bogachev, A., Finel, M., Morgan, J. E., Puustinen, A., Raitio, M., Verkhovskaya, M. & Verkhovsky, M. I. (1994). *Biochem. Biophys. Acta*, **1187**, 106–111.
Xia, D., Yu, C. A., Kim, H., Xia, J. Z., Kachurin, A. M., Zhang, L., Yu, L. & Deisenhofer, J. (1997). *Science*, **277**, 60–66.
Yoshikawa, S., Shinzawa-Itoh, K., Nakashima, R., Yaono, R., Yamashita, E., Inoue, N., Yao, M., Fei, M. J., Peters Libeu, C., Mizushima, T., Yamaguchi, H., Tomizaki, T. & Tsukihara, T. (1998). *Science*, **280**, 1723–1729.
Zhang, Z., Huang, L., Shulmeister, V. M., Chi, Y. I., Kim, K. K., Hung, L. W., Crofts, A. R., Berry, E. A. & Kim, S. H. (1998). *Nature (London)*, **392**, 677–684.